Proceedings of the 16th Czech and Slovak Conference on Magnetism, Košice, Slovakia, June 13–17, 2016

The Correlation between Magnetic and Structural Properties in Ni–Ti–Zr Metallic Glass

M. Lisnichuk[a], Yu. Katuna[a], K. Saksl[a,b], V. Girman[a], J. Gamcová[a,*], D. Balga[b], M. Ďurišin[b], J. Kováč[c], P. Kollár[a] and P. Sovák[a]

[a]Institute of Physics, Faculty of Science, P.J. Šafárik University, Park Angelinum 9, 041 54 Košice, Slovakia
[b]Institute of Materials Research, Slovak Academy of Sciences, Watsonová 47, 04001 Košice, Slovakia
[c]Institute of Experimental Physics of SAS, Watsonová 47, 040 01 Košice, Slovakia

The Ni–Ti–Zr metallic glasses are due to their known shape memory properties promising alloys e.g. for micromechanical applications. In this paper structure and structure stability of one particular alloy $Ni_{60}Ti_{25}Zr_{15}$ at.% were examined by means of X-ray diffraction and transmission electron microscopy while magnetic properties were ascertained by vibrating-sample magnetometer with maximal applied field of 100 kA/m in the temperature range of 300–1073 K.

DOI: 10.12693/APhysPolA.131.741
PACS/topics: 07.85.Jy, 75.50.Kj, 61.43.Dq

1. Introduction

Alloys consisting of Ni–Ti–Zr exhibit thermally stable structural and mechanical properties, good corrosion resistance and biocompatibility [1]. They are assumed to be one the most promising high-temperature shape memory alloys. The shape memory effect is consequence of thermoelastic structural changes between austenitic and martensitic phase [2], therefore the aim of our work was to investigate $Ni_{60}Ti_{25}Zr_{15}$ alloy from magnetic and structural point of view in amorphous state and after heat treatments processing.

2. Experiment

For the alloys preparation nickel, titanium and zirconium elements of high purity, all above 99.9%. was used. The Mini Arc Melting system MAM-1 was used for preparation of master alloy of $Ni_{60}Ti_{25}Zr_{15}$ in form of compact spherical shape. The master alloy was re-melted three times in protective Ar atmosphere in order to ensure homogeneous elements distribution within the whole alloy volume. From the master alloy amorphous ribbon was prepared by rapid solidification process (melt spinning). The alloy was heated to temperature 1930 K well above melting point of the alloy 1657 K followed by rapid quenching on surface of rotating Cu wheel with of surface velocity 1.57 m/s. As a result of the melt spinning we obtained the alloy in ribbon shape of thickness ≈ 60 μm and width ≈ 4 mm.

Magnetic properties were ascertain by vibrating sample magnetometer measuring the sample in as-quenched and *in situ* during heating.

Phase composition and structural state of the alloy in different stages were examined by X-ray diffraction (XRD) technique using the X'Pert PRO diffractometer with Cu anode radiation and by selected area electron diffraction (SAD) technique in transmission electron microscope JEOL JEM 2100F UHR equipped with the Schottky cathode and operated at acceleration voltage 200 kV.

3. Experiment results

XRD data taken from the as-quenched sample and the sample after selected heat treatments are shown in Fig. 1. Exact temperatures of heat treatments were chosen on the ground of different scanning calorimetry measurements of $Ni_{60}Ti_{25}Zr_{15}$ alloy performed in affined work [3]. As-quenched sample is fully amorphous (Fig. 1a) which is testified also by corresponding TEM image (Fig. 2a). After heating to 837 K, diffraction pattern consists of the Bragg peaks visible together with amorphous background. At 914 K another phase transformations are

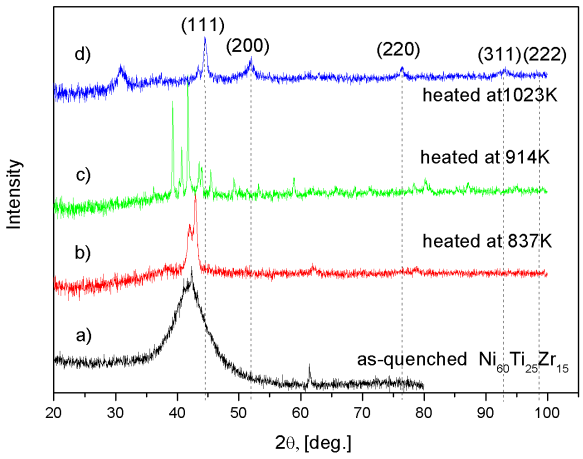

Fig. 1. XRD profiles of as-quenched $Ni_{60}Ti_{25}Zr_{15}$ (a) and heated to 837 K (b), 914 K (c), and 1023 K (d).

*corresponding author; e-mail: jana.gamcova@upjs.sk

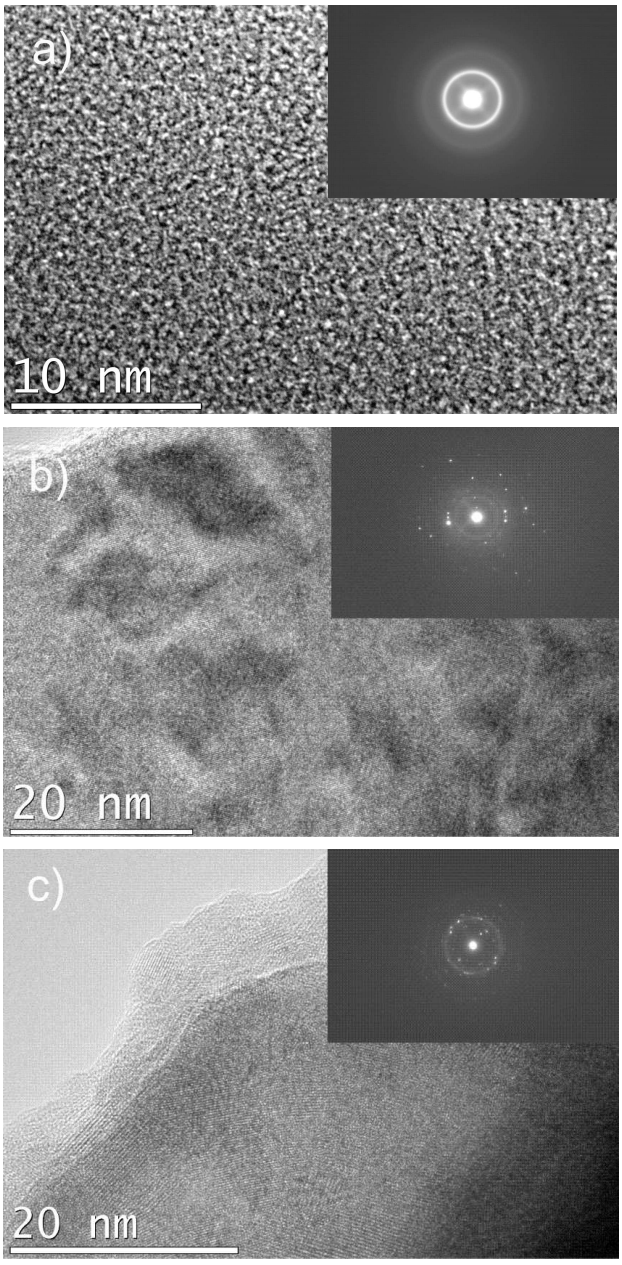

Fig. 2. Bright-field TEM imges and embedded diffraction pattern for the as-quenched (a), heated to 837 K (b), and heated to 914 K (c) $Ni_{60}Ti_{25}Zr_{15}$ alloy.

taking place distinguished by clear change of the corresponding XRD and TEM diffraction patterns. It was found that all transitions up to 914 K result into only very weak magnetic phases. At heating temperature 1023 K the third phase transition is observed. Dominant Bragg peaks on the pattern were indexed to pure nickel. This is in good agreement with magnetic measurement.

Bright field high-resolution TEM images also approve amorphous and crystalline structure state of as-quenched and heated samples, respectively. In order to estimate the size of crystallites fast Fourier transformation images processing was used. Filtering of corresponding frequency maxima left the only one crystallite clearly visualised and measured. Finally, size of crystallites in heated samples have been estimated as 17 nm for 837 K and 12 nm for 914 K samples.

Hysteresis loops, measured by the vibrating-sample magnetometer (VSM), confirmed paramagnetic behaviour of the as-quenched sample state.

The temperature dependence of saturation magnetization, measured by the same VSM, in constant magnetic field of 100 kA/m and at the heating rate 10 K/min is shown in Fig. 3. The VSM measurement consist of two parts heating from room temperature to 1073 K and cooling down from 1073 K to room temperature. During the cooling part of measurement increase of magnetization is observed with onset at temperature $\sim$ 640 K, which is typical ferromagnetic manifestation. The Curie temperature (T_C) related to this point was stated to be 631 K which is very close to well-known T_C of the pure nickel. From this measurement we can estimate that phase crystallized out of the amorphous precursor and responsible for ferromagnetic behaviour can be pure Ni.

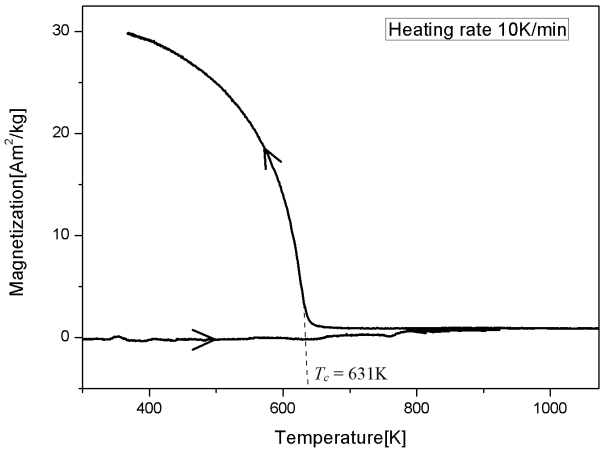

Fig. 3. Temperature dependence of saturation magnetization.

Based on the smooth profile of reverse curve it can be concluded that there is only one ferromagnetic phase which contributes to rising of magnetization. Additional calculations of magnetic polarization for pure nickel with respect to alloy composition ($J_{calc} = 0.639$ T) is in good accordance with its tabular value ($J_{tab} = 0.63$ T) [4]. After all, it can be drawn to close doubtlessly that responsible phase for paramagnetic-to-ferromagnetic transition is pure nickel.

Magnetic properties, obtained from hysteresis loops measured of samples pre-heated to significant temperatures, are listed in Table I. After thermal treatments to 815, 837, 891, and 914 K the sample has only low values of magnetization. However, after heating above 1023 K significant increase of magnetization (M_s), remanent magnetization (M_r) and coercive field (H_c) (measured at maximum magnetic field of 100 kA/m) was detected (see Table I).

TABLE I

Magnetic properties of $Ni_{60}Ti_{25}Zr_{15}$ ribbons after different thermal treatments.

T [K]	814	837	890	914	1023	1073
M_s [A m^2/kg]	0.29	0.65	0.56	0.66	22.5	34
M_r [A m^2/kg]	0.15	0.23	0.19	0.22	14.1	16.2
H_C [kA/m]	7	9.3	7.3	7.3	15	13.5

4. Conclusions

The $Ni_{60}Ti_{25}Zr_{15}$ at.% amorphous alloy was prepared by melt spinning — rapid solidification technique.

Both, magnetic properties and XRD patterns, were measured from the amorphous as-quenched and preheated crystallized samples. After first and second crystallization the sample undergoes phase transformation, but without any significant effect on the magnetic properties. Magnetic behavior of all samples was paramagnetic. The only paramagnetic-to-ferromagnetic transition was noticed during magnetic saturation measurements. Explanation of this observed phenomenon reclines upon segregation process of pure nickel from Ni–Ti–Zr intermetallic type structure, which may be considered interesting. The possibilities of its interpretation are more discussed in [3]. Nevertheless, the nickel segregation feature can be potentially utilized e.g. in preparation of pure nickel nanoparticles under controlled way (by dissolution of TiZr matrix) or by preparation of fine meshes (by dissolution of nickel particles).

Shape memory properties of the Ni–Ti–Zr type alloy is well described [5] but for lower content of zirconium. For this reason $Ni_{60}Ti_{25}Zr_{15}$ alloy will be matter of future investigation.

Acknowledgments

Authors would like to thank Prof. Rastislav Varga for valuable advice and help. This work was supported by the project VEGA 1/0036/16 and VEGA 2/0021/16. This work was realized within the frame of the project NanoCEXmat II (ITMS 26220120035) "Infrastructure Improving of Centre of Excellence of Advanced Materials with Nano- and Submicron- Structure", which is supported by the Operational Program "Research and Development" financed through European Regional Development Fund.

References

[1] P.J. McCluskey, J.J. Vlassak, *J. Mater. Res.* **25**, 2086 (2010).

[2] J. Ma, I. Karaman, R.D. Noebe, *J. Int. Mater. Rev.* **55**, 257 (2010).

[3] Yu. Katuna, M. Lisnichuk, K. Saksl, V. Girman, J. Gamcová, D. Balga, M. Ďurišin, J. Kováč, P. Sovák, *Acta Phys. Pol. A* **131**, 750 (2017).

[4] S. Tumanski, *Handbook of Magnetic Measurements*, CRC Press, Boca Raton 2011.

[5] K. Otsuka, X. Ren, *J. Prog. Mater. Sci.* **50**, 511 (2005).